Mater. Res. Soc. Symp. Proc. Vol. 1766 © 2015 Materials Research Society
DOI: 10.1557/opl.2015.424

Effect of Li-doping on Photoluminescence of Screen-printed Zinc Oxide Films

L. Khomenkova[1], V. Kushnirenko[1], M. Osipenok[1], K. Avramenko[1], Y. Polishchuk[1], I. Markevich[1], V. Strelchuk[1], V. Kladko[1], L. Borkovska[1] and T. Kryshtab[2]

[1] V. Lashkaryov Institute of Semiconductor Physics of NAS of Ukraine,
Pr. Nauky 41, 03028 Kyiv, Ukraine
E-mail: khomen@ukr.net

[2] IPN – ESFM, Av. IPN, Edificio 9 U.P.A.L.M. C.P. 07738 México
E-mail: kryshtab@gmail.com

ABSTRACT

Undoped and Li-doped ZnO films were fabricated by screen printing approach on sapphire substrate. The effect of Li doping and annealing temperature on the luminescent, optical, electrical and structural properties of the films has been investigated by the photoluminescence (PL), Raman scattering, conductivity, Atomic Force microscopy and X-ray diffraction (XRD) methods. The XRD study revealed that the films have polycrystalline wurtzite structure with grain sizes ranging from 26 to 38 nm. In the undoped ZnO films, the increase of annealing temperature from 800 to 1000 °C resulted in the increase of the grain sizes, film conductivity and the intensity of the ultraviolet PL. The introduction of Li of low concentration of 0.003 wt % at 800 °C or 900 °C allows producing the low-resistive films with enhanced ultraviolet PL and reduced density of crystalline defects. Highly doped films (with 0.3 wt % of Li) were found to be semi-insulating with deteriorated PL properties irrespectively of the annealing temperature. It is shown that introduction of Li in the ZnO films affects their PL spectra mainly via the evolution of the film crystallinity and the density of intrinsic defects.

INTRODUCTION

Over the past decades, ZnO-based materials have been attracted considerable attention for possible application in optoelectronic devices, especially to ultraviolet (UV) light emitters [1]. The structural, optical and electrical properties of ZnO films can be governed by dopants, deposition parameters and post-treatments. Doped ZnO films are of great interest for their applications in transparent conducting electrodes for solar cells and displays [2, 3] and insulating or ferroelectric layers for optical memory devices [4]. However, hardly achievable p-type conductivity of ZnO-related materials remains the drawback for their wide applications.

The large efforts were applied to obtain p-type ZnO by doping with elements of groups I (Li, Na, K) or V (N, P, As) as well as by their co-doping [1]. Among these, lithium (Li) has been considered as a promising dopant for ZnO [5-8] in spite of rather contradictory viewpoints on realization of stable p-type activity under equilibrium conditions.

As a rule, Li-doping occurs as follows [9]:

$$Li_2O \xrightarrow{ZnO} Li_{Zn}^{-} + Li_i^{+} + O_O \qquad (1)$$

Where Li_{Zn}^{-} represents lithium on zinc lattice site, Li_i^{+} is a lithium in interstitial position, and O_O is an oxygen on its lattice site.

The most of experimental reports supposed that Li_{Zn} is a deep acceptor with a binding energy of about 800 meV responsible for luminescence band peaked at 2.0-2.2 eV [10-13]. However, it was theoretically predicted that Li_{Zn} produces shallow acceptor level [14]. In fact, in some luminescent studies of Li-doped ZnO materials, the shallow acceptor states having binding energies of about 300 meV were demonstrated and ascribed to Li_{Zn} defects [15, 16]. These shallow acceptor states are responsible for luminescence band around 3.05 eV and are introduced only if the growth/diffusion temperature is below 700 °C, otherwise deep acceptor state (with the 800 meV binding energy) is formed [16]. The amphoteric behavior of Li in the ZnO together with an ability of Li_{Zn} acceptor to form neutral complexes with other defects has been suggested to be responsible for semi-insulating nature of ZnO:Li materials [4, 10].

Furthermore, if Li-doping is performed during ZnO crystallization, lithium can affect also the crystallinity of ZnO films. These data are also rather contradictory. Specifically, the X-ray diffraction (XRD) study of Li-doped ZnO films and ZnO powders has shown that Li introduction upon thermal annealing can suppress [17, 18] and/or promote [7, 8, 17, 18] the growth of nanocrystals in sizes. Besides, Raman scattering investigations of Li-doped ZnO revealed that Li can stimulate [19] or counteract [20, 21] the formation of point defects presumably the oxygen vacancies or Zn interstitials. However, the effect of Li on the film crystallinity usually is not taking into account when the role of Li_{Zn} acceptor in the photoluminescence (PL) of ZnO is considered.

In this work we have studied the effect of Li on the PL of ZnO thick films prepared by a screen printing method and doped with Li at different annealing temperatures. In addition, the influence of Li doping on the film crystallinity have been analyzed.

EXPERIMENTAL

The 40-μm films of undoped and Li-doped ZnO (ZnO: Li) were produced by the screen printing method on (1012) sapphire substrates of 10x10x0.5 mm^3 dimension using ZnO-based paste (Fig.1). The paste was made from the ZnO powder (Sigma-Aldrich, 99.99%) crushed in a ball mill for 125 h and mixed with distillate water or with $LiNO_3$ aqueous solution.

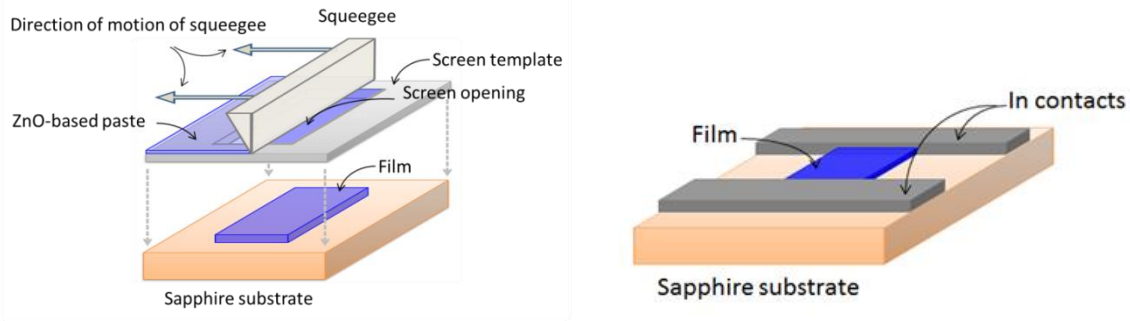

Figure 1. Schematic illustration of screen-printing technique used for ZnO films fabrication (left) and the sample with In contacts prepared by thermal evaporation with shadow mask (right).

The paste was distributed on the non-flexible template with opening places and then pushed towards a sapphire substrate using motion of the squeegee along the template. More details about fabrication approach can be found in [22]. After template removing, the films with required configuration were obtained on the substrate. As-printed films were dried at normal conditions for 24 h and then annealed in air at 800, 900 and 1000 °C for 30 min in muffle furnace. The Li concentrations in dried doped films were 0.003, 0.03 and 0.3wt %.

The PL and PL excitation (PLE) spectra were studied both at room and at liquid-nitrogen temperatures, whereas all other experiments were performed at room temperature only. The PL was excited by a 337.1 nm line of pulsed N_2-laser or by a light of Xe-lamp passed through a grating monochromatic. Atomic Force microscopy (AFM) was used to investigate the morphology of the films. The study of film surface was performed using NanoScope IIIa Dimension 3000TM (Digital Instruments). Measurements were carried out in contact mode using silicon probes (NT-MDT brand NSG01) with a tip radius of about 10 nm. The Raman scattering spectra were excited with a 488.0 nm line of an Ar-Kr ion laser and collected by a triple Raman spectrometer T-64000 Horiba Jobin-Yvon with a resolution about 0.15 cm^{-1}. XRD study was realized using X-ray powder diffractometer ARL X'TRA with the Cu $K\alpha_1$ and Cu $K\alpha_2$ radiation. For electric measurements, indium strip-like contacts were fabricated by thermal evaporation of pure In (99, 9%) onto the surface of ZnO film through shadow mask (Fig.1). Dark current-voltage characteristics were measured in the range of 1-40 V of applied bias, demonstrating linear behavior. To investigate photoelectric properties of the films, ultraviolet emission of a 500 W Hg lamp was used as excitation source.

RESULTS AND DISCUSSION

Morphology characterization

To obtain the information about sintering process of ZnO-based films, the surface morphology of the films was investigated by means of AFM method before and after annealing. Figure 2 represents three-dimensional AFM images obtained in tapping mode for as-printed dried film (Fig. 2a) and after film annealing at 1000 °C (Fig. 2b). It is seen that the surface of as-printed dried films consists of polycrystalline aggregates of ZnO grains with lateral dimensions in the range of 140-1800 nm and vertical dimensions within 50-1200 nm.

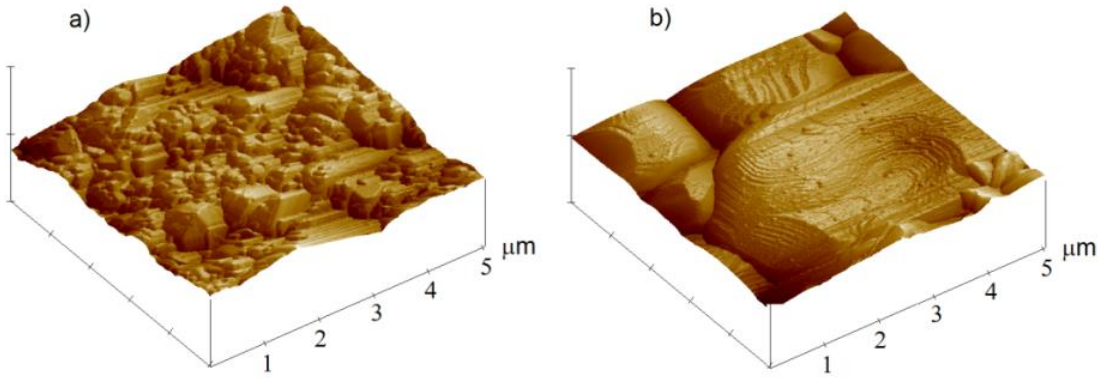

Figure 2. Three-dimensional AFM topography image of the surface of zinc oxide films obtained before (a) and after (b) annealing treatment at 1000 °C.

Smaller ZnO grains have fuzzy-like grain boundaries, whereas large grains demonstrate well organized layer-like structure. This is demonstrated by the appearance of the terraces with the height of 50-100 nm (Fig. 2a). After film sintering at 800-1000 °C, the recrystallization of the films was observed. As one can see from Fig. 2b, a significant increase of the external lateral and vertical dimensions of ZnO grain occurs. This process depends on the annealing conditions and for the samples annealed at 1000 °C, the grain size was found to be larger than 2 μm (Fig. 2b). In some cases the formation of the grains with the sizes up to 30 μm was observed (not shown here).

The Li-doped ZnO films sintering at different conditions were also investigated by AFM method. However, no significant difference was found in comparison with undoped films. The external dimensions of the ZnO grains were found to be in the range 0.5-2 μm that were similar to those obtained for undoped films, especially when the films were annealed at lower temperature. Based on this morphology observation, one can assume that during sintering the main transformation occurs inside large ZnO grains that has to affect optical, electrical and luminescent properties of the films.

Photoluminescence investigations

The room-temperature PL spectra of the ZnO and ZnO:Li films are shown in Figure 3. In the spectra, an UV PL band (I_{UV}) and a wide defect-related PL band (I_{DEF}) in the green-orange spectral range can be observed. Both the intensity and spectral position of these bands depend on the annealing temperature and Li concentration.

In the undoped ZnO films annealed at 800 °C and 900 °C, an intensity of the UV band is strongly reduced. It increases noticeably after the film annealing at 1000 °C. In the Li-doped films with the lowest Li concentration (0.003 wt%), strongly enhanced UV emission is observed already upon the annealing at 800 and 900 °C, but in the films with the highest Li concentration (0.3 wt%), no exciton emission is detected irrespective of the annealing temperature. In the last case the intensity of the visible defect-related band is found to be reduced too.

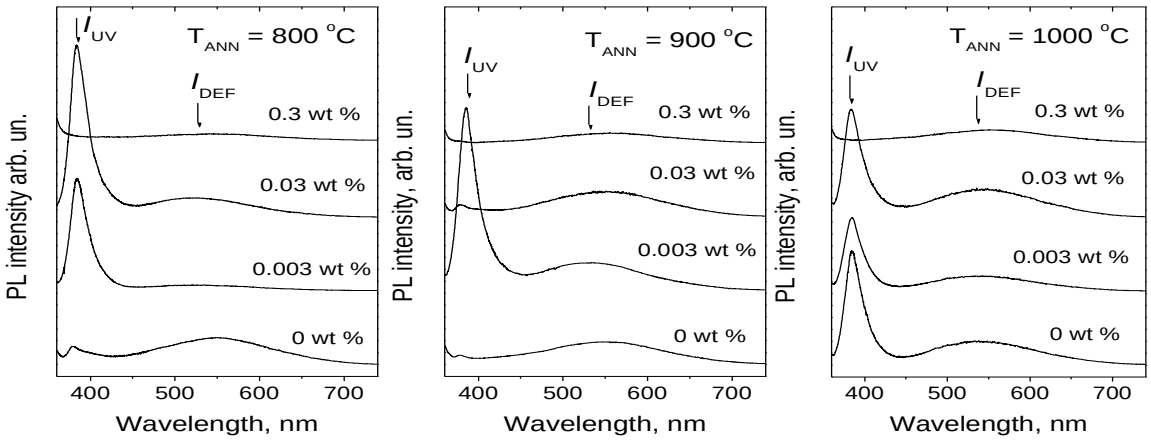

Figure 3. Room-temperature PL spectra of undoped and Li-doped ZnO films with different content of Li (0, 0.003, 0.03 and 0.3 wt %) annealed at 800 °C, 900 °C, 1000 °C for 30 min.

It should be noted, that in both undoped and Li-doped samples, spectral position of the I_{UV} band changes from 378 nm in the films with low intensity of this band to 384 nm in the films with strongly enhanced UV PL. In turn, spectral position of the maximum of the I_{DEF} band varied in the range of 522-555 nm in different samples and showed the shortest wavelength position in the ZnO:Li films doped with Li of 0.003 wt% and 0.03 wt% and annealed at 800 °C.

In the low-temperature PL spectra of the ZnO and ZnO:Li films (Fig. 4a) the same I_{UV} and I_{DEF} PL bands are present. Figure 4b shows the ratio of the intensity of the UV band to the intensity of the visible defect-related band that is usually considered for simple estimation of structural defects in ZnO. Similarly to room-temperature PL spectra, the best PL characteristics are observed in Li-doped films with low Li concentration, while the worth PL properties are found for highly doped ZnO:Li films (no UV emission). An enhancement of the relative intensity of the UV PL caused by Li introduction is observed: in the films annealed at 800 °C for 0.003 and 0.03 wt % of Li, in the films annealed at 900 °C for 0.003 wt % of Li only, while in the films annealed at 1000 °C no improvement of the UV PL is found.

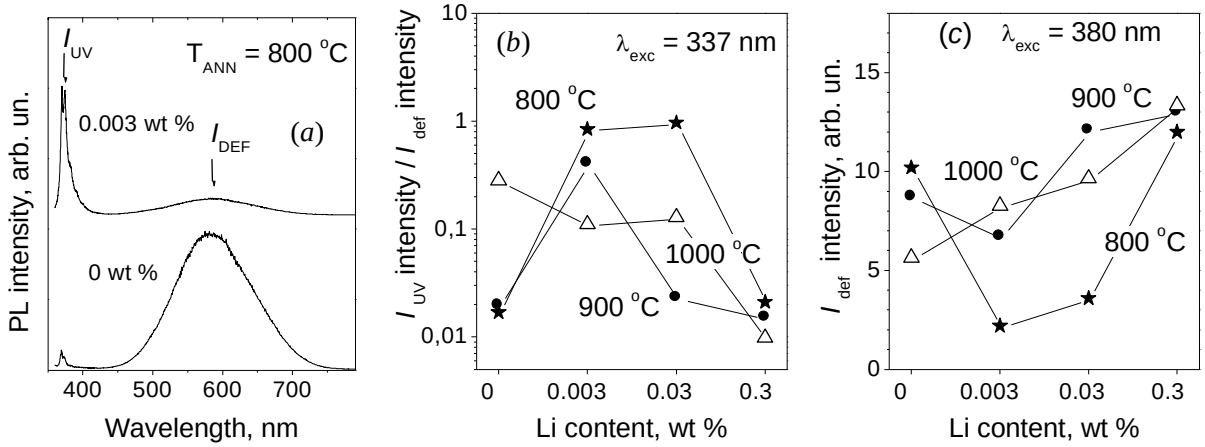

Figure 4. Low-temperature PL study: (a) PL spectra of annealed at 800 °C undoped ZnO and ZnO:Li (0.003 wt %) films under N_2-laser excitation; (b) Ratio of integrated intensities of the I_{UV} to the I_{DEF} band versus Li content; (c) Intensity of the I_{DEF} band under defect-related excitation versus Li content.

At low-temperature, the visible defect-related PL band shifts towards longer wavelengths and its maximum is found to be peaked at about 580-590 nm (Fig. 4a). This indicates that this PL band is complex and composes of at least two overlapped PL bands peaked at 520 nm ("green") and 590 nm ("orange"). At low temperatures, the "orange" PL component dominates, while at room temperature the "green" one contributes mainly to I_{DEF}. In the undoped ZnO films, these PL bands are usually assigned to intrinsic defects, such as the Zn vacancy (V_{Zn}), interstitial zinc (Zn_i), the O vacancy (V_O), oxygen antisite (O_{Zn}), etc. [1,23-25]. In spite of the fact that the "orange" band is often ascribed to Li_{Zn} acceptor we cannot exclude that in the ZnO:Li films this band originates from the intrinsic defects of ZnO mainly. This is because neither a pronounced increase in the intensity, nor the evident shift of the I_{DEF} peak position are observed in the ZnO:Li films as compared with the undoped films.

In the PLE spectra of "orange" PL component (recorded at 630 nm to eliminate the contribution of "green" PL component), in addition to a small peak at 369 nm corresponding to generation of exciton, a wide maximum at 380-385 nm is found (Fig. 5). The maximum at 385 nm is not observed in the PLE spectra of "green" PL component (recorded at 520 nm) and it is apparently caused by some defect-related absorption.

In the ZnO films annealed at 800 and 900 °C as well as in all ZnO:Li films with the highest Li content, the intensity of "orange" PL component under defect-related excitation (λ_{exc}=380 nm) exceeds that under band-to-band excitation. Figure 4c shows that, in general, in the ZnO:Li films, the intensity of "orange" PL band under defect-related excitation increases both with the increase of Li concentration and the annealing temperature. This means that introduction of Li stimulates the formation of intrinsic defects or their complexes with Li ions.

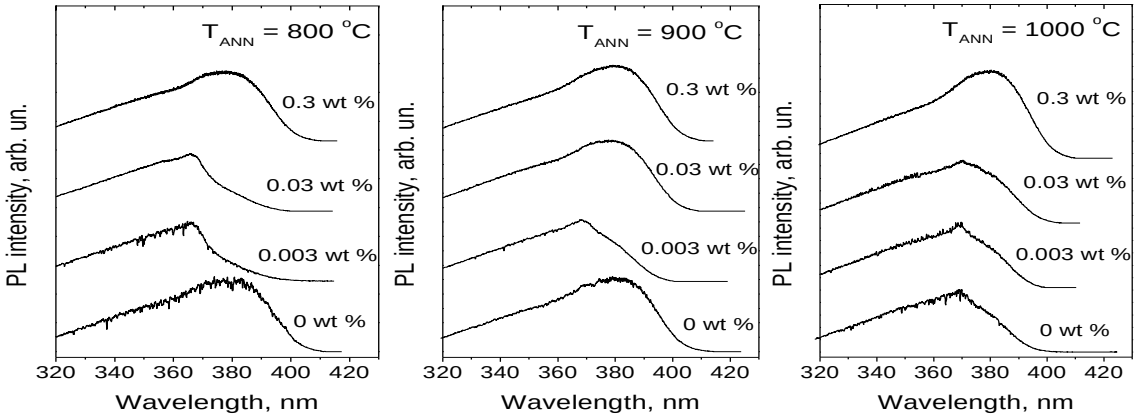

Figure 5. Liquid-nitrogen PL excitation spectra of defect-related PL band in undoped and Li-doped ZnO films with different Li content (0, 0.003, 0.03 and 0.3 wt %) annealed at 800 °C, 900 °C, 1000 °C for 30 min. The spectra are recorded at λ_{PL}=630 nm and normalized to the PL intensity at 337 nm.

Raman scattering spectroscopy

The Raman spectra of undoped and Li-doped films show wurtzite structure of the ZnO (Fig. 6). By comparison with the assignments of pure ZnO, Raman peaks at 99, 332, 379, 410 and 438 cm^{-1} correspond to E_2^{low}, E_2^{high}-E_2^{low}, A_1(TO), E_1(TO) and E_2^{high} modes, respectively [26].

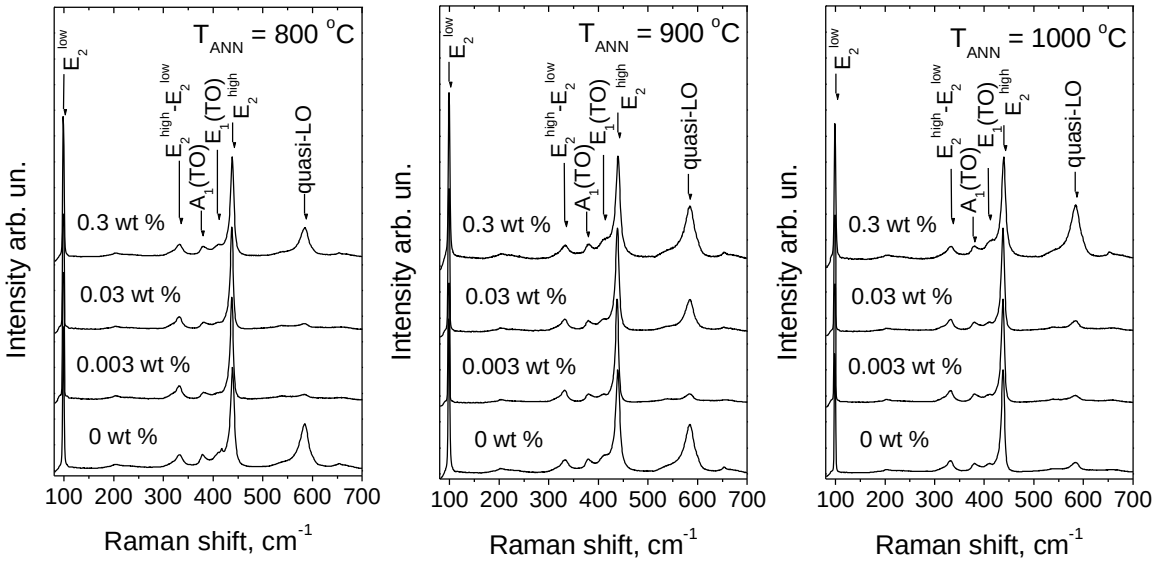

Figure 6. Room-temperature Raman spectra of undoped and Li-doped ZnO films with different content of Li (0, 0.003, 0.03 and 0.3 wt %) annealed at 800 °C, 900 °C, 1000 °C for 30 min. Raman active modes are indicated. The spectra are normalized on the intensity of E_2^{high} mode. λexc=488.0 nm.

The peak at 584 cm^{-1} marked as a quasi-LO mode lies at an intermediate frequency between the A_1(LO) and E_1(LO) modes and is ascribed to a quasi-mode of mixed A_1 and E_1 symmetry. Both the change in the annealing temperature and Li-doping affect the characteristics of E_2^{high} mode associated with oxygen-atom vibrations in ZnO lattice (Fig. 7a, b). Specifically, in the undoped ZnO films annealed at 800 and 900 °C as well as in highly doped ZnO films, the E_2^{high} mode is found to be broadened and shifted towards higher frequencies (up to 439 cm^{-1}) as compared with the bulk value of 437 cm^{-1}. This testifies to a decrease of lattice parameters in ZnO nanocrystals, which can be caused by external compressive stress, the presence of vacancy-related defects or Li incorporation in the Zn sublattice.

In Raman spectra of ZnO:Li films with 0.003 wt % of Li annealed at 800 °C and 900 °C, a low frequency shift and a decrease of a full width at a half maximum (FWHM) of the E_2^{high} mode are observed indicating strain relaxation and improvement of oxygen sublattice crystal structure (Fig. 7b). Further increase of Li concentration produces a reverse trend in the spectral shift and FWHM of the E_2^{high} mode.

The appearance of the quasi-LO mode in the Raman spectra has been attributed to the structural disorder in the ZnO such as V_O, Zn_i or their complexes [27]. Figure 7c shows that in the undoped ZnO films annealed at 800 and 900 °C, intensity of the quasi-LO mode is high and reduces in the film annealed at 1000 °C. This indicates the decrease of structural disorder in the films annealed at higher temperatures. At the same time, in the ZnO:Li films with lower Li concentration, the quasi-LO mode become weak that testifies to the decrease of density of structural defects owing to Li incorporation. However, all films with the highest Li concentration demonstrate enhanced quasi-LO mode. This means that introduction of high amount of Li produces additional structural disordering.

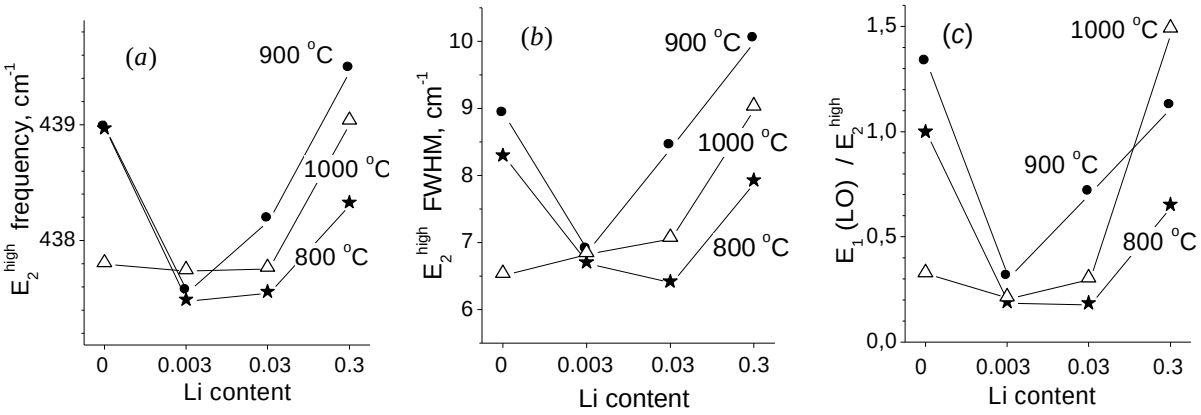

Figure 7. Peak position (a) and FWHM (b) of the E_2^{high} mode as well as integrated intensity ratio of the quasi-LO and E_2^{high} modes (c) versus Li content in the film annealed at different temperatures: 800 °C (stars), 900 °C (circles), 1000 °C (triangles).

Photo- and dark conductivity investigation

The results of conductivity investigation in the undoped and Li-doped films are summarized in Figure 8. The lowest conductivity was found in the undoped films annealed at 800 and 900 °C as well as in all ZnO:Li films with the highest Li content. In turn, the ZnO film annealed at 1000 °C as well as the ZnO:Li films with the lowest Li content (0.003 wt%) demonstrate a hundredfold larger dark and photo-conductivities.

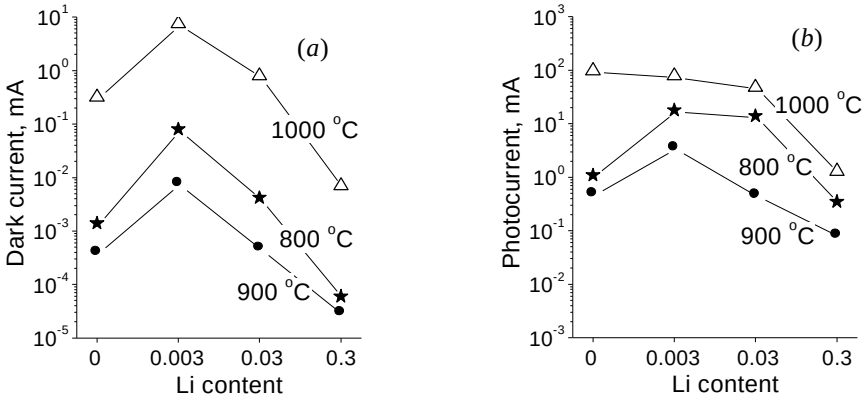

Figure 8. Room-temperature dark (a) and photo- (b) conductivities of undoped and Li-doped ZnO films annealed at 800 °C (stars), 900 °C (circles), 1000 °C (triangles) versus Li content. U=9 V.

X-ray diffraction study

The XRD patterns of undoped and Li-doped ZnO films show the peaks corresponded to polycrystalline wurtzite ZnO without preferable grain orientation (Fig. 9a). The marked extra peaks are due to the contacts. In the undoped films, the increase of annealing temperature leads to the shift of XRD peaks towards the lower angles and the decrease of peak FWHM indicating

the increase of ZnO lattice parameters and grain size, respectively (Fig. 9a). The same effect is observed in the ZnO:Li film with the lowest Li content annealed at 800 °C. At the same time for ZnO:Li films with the highest Li content the diffraction peaks shift towards larger angles and FWHM increases. Assuming a homogeneous strain across the films, the crystallite sizes were evaluated from FWHM for different XRD peaks using the Scherrer equation. The representative behavior of grain sizes in dependence on annealing temperature and Li content is shown in Figure 9b for (002) diffraction peak.

In the undoped ZnO films, the crystallite sizes increase from 26 to 38 nm when the annealing temperature increases. In polycrystalline ZnO films, it is assumed that at higher temperatures the atoms have enough activation energy to occupy the proper sites in the crystal lattice, and larger grains with lower surface energy are formed [28]. The introduction of Li of low concentration also promotes nanocrystal growth at low temperatures while the highest Li content hinder this process (Fig.9b). The nonmonotonic dependence of the ZnO grain sizes on Li content in the ZnO:Li films has been observed also in [8, 17]. It has been supposed that diffusivity of the interstitial zinc, which is considered to play an important role in the grain growth of ZnO, is higher in the Li-doped ZnO than in the undoped one, because Li^+ has a smaller ionic radius of 0.060 nm than Zn^{2+} having 0.074 nm [8]. This can explain the increase of grain size in the films with low Li content. The decrease of grain size in the films with the highest Li content can be caused by segregation of insoluble Li atoms at the grain boundaries, which suppress the growth of nanocrystals [18]. In fact, the redundant Li elements congregated as the second phases on the grain boundaries of ZnO nanocrystals has been revealed by high resolution X-ray photoelectron microscopy in Li-doped ZnO powders with Li content of about 5 at % [7]. The dependence presented in Fig. 9b indicates that not only Li content but also the annealing temperature is important for the ultimate effect of Li doping on the grain growth.

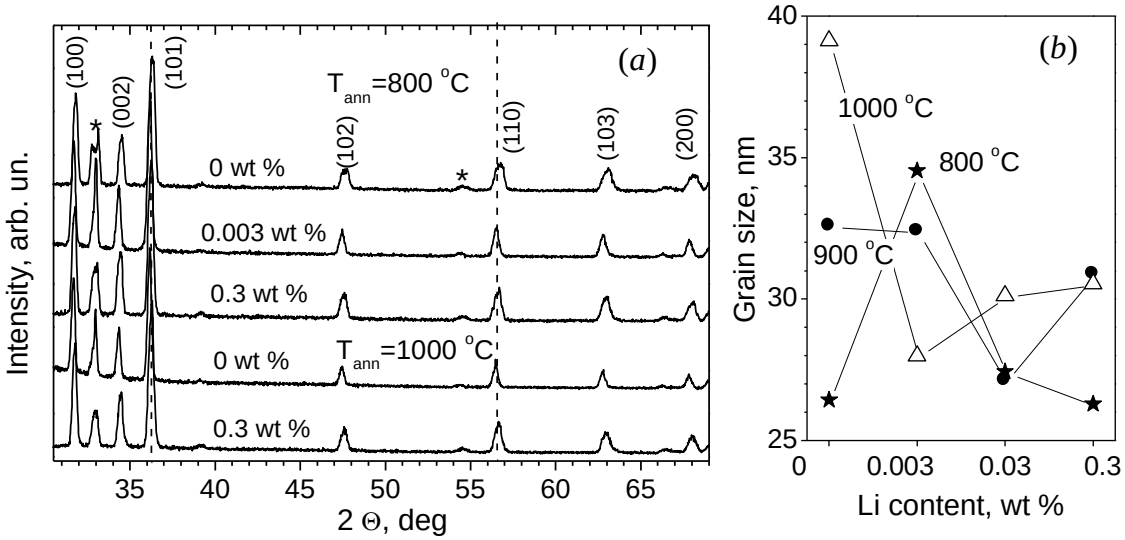

Figure 9. XRD patterns (a) and grain sizes (b) of undoped and Li-doped ZnO films vs Li concentration and annealing temperature. The peaks marked with * are caused by contact.

The increase of crystal sizes is accompanied by the improvement of PL and optical characteristics as well as by the increase of film conductivity and vice versa, although this interconnection is not so direct. The increase of crystal sizes decreases the density of intercrystalline boundaries, which act as the sinks for point defects, in particular, for oxygen

ions. The oxygen ions chemisorbed at the film surface and at the grain boundaries are known to be the origin of low dark conductivity in undoped polycrystalline ZnO films [29]. Therefore, higher dark conductivity in the films with larger crystal sizes is seemingly connected with the decrease of extended defects, though the appearance of Li_i donors in the ZnO:Li films can increase conductivity too. A fairly good correlation of the PL characteristics (relative intensity of the UV PL, the appearance of the defect-related maximum in the PLE spectra) and optical properties (the characteristics of the E_2^{high} mode, the appearance of the quasi-LO mode in the Raman spectra) is found. This allows supposing that modification of the ZnO films microstructure caused by Li introduction affects also the formation of vacancy and interstitial defects inside the crystals as well as stimulate the defect diffusion during crystal growth.

CONCLUSIONS

The present work demonstrates the utility of screen printing technique for the fabrication of undoped and Li-doped ZnO films. The films annealed at 800-1000 °C were found to be polycrystalline of wurtzite structure. The undoped ZnO films showed the increase of the grain sizes and the decrease of the concentration of crystalline defects with the increase of the annealing temperature. The improvement of the films crystallinity was accompanied by an increase of the intensity of the UV PL and both dark- and photo-conductivities. The effect of Li on the films crystallinity as well as on the PL and electrical properties was found to depend not only on Li content but also on the annealing temperature. The doping with low Li concentration (0.003 wt%) at 800 °C allowed producing the films with improved characteristics and thus decreasing thermal budget for film production. On the contrary, highly doped films (0.3 wt% of Li) were found to be semi-insulating, having smaller crystal sizes and a lot of crystalline defects that result in dramatic quenching of the UV PL. It is shown that the effect of Li-doping on both UV and visible defect-related PL bands appears mainly in the influence of Li on the development of film microstructure via the control of crystal sizes and concentration of native point defects.

ACKNOWLEDGMENTS

This work was supported by National Academy of Sciences of Ukraine via the project III-10-12 and by CONACYT, Mexico.

REFERENCES

1. Ü. Özgür, Ya. I. Alivov, C. Liu, A. Teke, M.A. Reshchikov, S. Doğan, V. Avrutin, S.J. Cho, H. Morkoç, *J. Appl. Phys.*, **98**, 041301 (2005).
2. T. Minami, H. Nanto, S. Takata, *Jpn. J. Appl. Phys*., **23**, L280 (1984).
3. J. Hu, R.G. Gordon, *Solar Cells* **30**, 437 (1991).
4. M. Joseph, H. Tabata, T. Kawai, *Appl. Phys. Lett.*, **74**, 2534 (1999).
5. S.H. Jeong, B.N. Park, S.B. Lee, J.H. Boo, *Thin Solid Films*, **516**, 5586 (2008).
6. M. Caglar, Y. Caglar, S. Aksoy, S. Ilican, *Appl. Surf. Sci.***, 256**, 4966 (2010).
7. B. Wang, L. Tang, J. Qi, H. Du, Zh. Zhang, *J. Alloys Compd.*, **503**, 436 (2010).
8. Sh. Fujihara, Ch. Sasaki, T. Kimura, *J. Eur. Ceram. Soc.*, **21**, 2109 (2001).
9. P. Bonasewicz, W. Hirschwald, G. Neumann, *J. EIectrochem. Soc.*, **133**, 2270 (1986).
10. W. Water, S.Y. Chu, Y.D. Juang, S.J. Wu, *Mater. Lett*., **57**, 98 (2002).

11. C. Rauch,W. Gehlhoff, M.R. Wagner, E. Malguth, G. Callsen, R. Kirste, B. Salameh, A. Hoffmann, S. Polarz, Y. Aksu, M. Driess, *J. Appl. Phys.*,**107**, 024311 (2010).
12. V.I. Kushnirenko, I.V. Markevich, T.V. Zashivailo, *J. Lumin* **132**, 1953 (2012).
13. N. Ohashi, N. Ebisawa, T. Sekiguchi, I. Sakaguchi, Yo Wada, *Appl. Phys. Lett.*, **86**, 091902 (2005).
14. M.G. Wardle, J.P. Goss, P.R. Briddon, *Phys. Rev. B*, **71**, 15520 (2005).
15. Z. Zhang, K.E. Knutsen, T. Merz, A.Yu. Kuznetsov, B.G. Svensson, L.J. Brillson, Appl. Phys. Lett., **100**, 042107 (2012).
16. B.K. Meyer, J. Stehr, A. Hofstaetter, N. Volbers, A. Zeuner, J. Sann, *Appl. Phys. A*, **88**, 119 (2007).
17. D.Y. Wang, J. Zhou, G.Z. Liu, *J. Alloys Compd*., **481**, 802 (2009).
18. P. Chand, A. Gaura, A. Kumar, U.K. Gaur, *Ceramics Intern.* **40**, 11915 (2014).
19. Y.L. Du, Y. Deng, M.S. Zhang, *Sol. St. Commun*, **137**, 78 (2006).
20. R. Yousefi, A. Khorsand.Zak, F. Jamali-Sheini, *Ceramics Intern*, **39**, 1371 (2013).
21. C. Bundesmann, N. Ashkenov, M. Schubert, D. Spemann, T. Butz, E.M. Kaidashev, M. Lorenz, M. Grundmann, *Appl. Phys. Lett.*, **83**, 1974 (2003).
22. M. Osipyunok, G. Pekar, O. Syngaivskyy, *The method of fabrication of solid layers by screen printed approach*, Patent of Ukraine 94561 (10.05.2011).
23. C. Ton That, L. Weston, M.R. Phillips, *Phys. Rev. B*, **86**, 115205 (2012).
24. A.F. Kohan, G. Ceder, D. Morgan, *Phys. Rev. B*, **61**, 15019 (2000).
25. M. Liu, A.H. Kitai, P. Mascher, *J. Lumin.*, **54**, 35 (1992).
26. J.M. Calleja, M. Cardona, *Phys. Rev. B*, **16**, 3753 (1977).
27. J.N. Zeng, J.K. Low, Z.M. Ren, T. Liew, Y.F. Lu, *Appl. Surf. Sci.*, **197**, 362 (2002).
28. Z.B. Fang, Z.J. Yan, Y.S. Tan, X.Q. Liu, Y.Y. Wang, *Appl. Surf. Sci.*, **241**, 303 (2005).
29. S.A. Studenikin, N. Golego, M. Cocivera, *J. Appl. Phys.*, **87**, 2413 (2000).